Direct UV-written broadband directional planar waveguide couplers

Massimo Olivero*, Mikael Svalgaard

COM, Technical University of Denmark, 2800 Lyngby, Denmark,
Phone: (+45) 4525 5748, Fax: (+45) 4593 6581,
svlgrd@com.dtu.dk

**Presently at PhotonLab, Politecnico di Torino, 10129 Torino, Italy,*
Phone: (+39) 011 2276301, Fax:(+39) 011 2276309,
massimo.olivero@polito.it

Abstract: We report the fabrication of broadband directional couplers by direct UV–writing. The fabrication process is shown to be beneficial, robust and flexible. The components are compact and show superior performance in terms of loss and broadband operation.

OCIS codes: (230.1360) Beam splitters; (130.3120) Integrated optics devices; (250.5300) Photonic integrated circuits; (060.2340) Fiber optics components; (160.5320) Photorefractive materials; (230.7390) Waveguides, planar; (350.4600) Optical engineering; (260.7190) Ultraviolet.

References and Links

1. R. Syms, J. Cozens, "Coupled mode devices," in *Optical Guided Waves and Devices*, (McGraw-Hill International Ltd., 1992), pp. 1-31.
2. Standard ITU-G 983.1 "Broadband optical access systems based on Passive Optical Networks (PON)" (International Communication Union, January 2005), http://www.itu.int/rec/recommendation.asp?type=products&lang=e&parent=T-REC-G.
3. J. P. Berger, P. Haguenauer, P. Kern, K. Perraut, F. Malbet, S. Gluck, L. Lagny, I. Schanen, L. Laurent, A. Delboulbe, E. Tatulli, W. Traub, N. Carleton, R. Millan-Gabet, J. D. Monnier, F. Pedretti, S. Ragland, "An integrated-optics 3-way beam combiner for IOTA," Proc. SPIE **4838**, 1099-1106 (2003).
4. A. Takagi, K. Jinguji, M. Kawachi, "Broadband silica–based optical waveguide coupler with asymmetric structure," Electron. Lett. **26**, 132-133, (1990).
5. K. Jinguji, N. Takato, A. Sugita, M. Kawachi, "Mach–Zender interferometer type optical waveguide coupler with wavelength–flattened coupling ratio," Electon. Lett. **26**, 1326-1327, (1990).
6. A. Takagi, N. Takato, Y. Hida, T. Oguchi, T. Nozawa, "Silica-based line-symmetric series-tapered (LSST) broadband directional coupler with asymmetric guides only in their parallel coupling regions," Electron. Lett. **32**, 1700-1702, (1996).
7. C. R. Doerr, M. Cappuzzo, E. Chen, A. Wong-Foy, L. Gomez, A. Griffin, L. Buhl, "Bending of a Planar Lightwave Circuit 2×2 Coupler to Desensitize it to Wavelength, Polarization, and Fabrication Changes," IEEE Photonics Technol. Lett. **17–6**, 1211-1213 (2005).
8. M. Svalgaard, C. V. Poulsen, A. Bjarklev, and O. Poulsen, "Direct UV-writing of buried single-mode channel waveguides in Ge-doped silica films," Electron. Lett. **30**, 1401-1402, (1994).
9. L. Leick, "Fabrication and characterization," in *Silica–on–silicon optical couplers and coupler based optical filters*, (PhD thesis, COM–Technical University of Denmark, 2002), pp. 28-30.
10. Lasse Leick, Ignis Photonyx A/S, blokken 84, 3460, Birkerød, Denmark (private communication, 2005).
11. G.D. Maxwell, B.J. Ainslie, "Demonstration of a directly written directional coupler using UV induced photosensitivity in a planar silica waveguide," Electron. Lett. **31**, 1694-1695, (1995).
12. D. Zauner, K. Kulstad, J. Rathje, M. Svalgaard, "Directly UV written silica–on–silicon planar waveguides with low insertion loss," Electron. Lett. **34**, 1582-1584, (1998).
13. P. J. Lemaire, R. M. Atkins, V. Mizrahi, W.A. Reed, "High pressure H_2 loading as a technique for achieving ultrahigh UV photosensitivity and thermal sensitivity in GeO_2 doped optical fibres," Electon. Lett. **29**, 1191-1193 (1993).
14. Svalgaard M., Færch K., Andersen L.U., "Variable Optical Attenuator Fabricated by Direct UV Writing," J. Lightwave Technol. **21–9**, 2097-2103, (2003).
15. M. Svalgaard, "Effect of D_2 outdiffusion on direct UV writing of waveguides," Electron. Lett. **35**, 1840-1841, (1999).
16. Renishaw tutorial, http://www.renishaw.com/UserFiles/acrobat/UKEnglish/GEN-NEW-0117.pdf

#8556 - $15.00 USD Received 23 August 2005; Revised 27 September 2005; Accepted 29 September 2005

17. Newport tutorial, http://www.newport.com/servicesupport/Tutorials/default.aspx?id=143
18. R.A. Betts, F. Lui, T.W. Whitbread, "Non destructive two-dimensional refractive index profiling of integrated optical waveguides by an interferometric method," Appl. Opt. **30**, 4384-4389, (1991).
19. T. Erdogan, V. Mizrahi, P. J. Lemarie, D. Monroe, "Decay of ultra−violet−light induced Bragg gratings," J. Appl. Phys. **76**, 73-80, (1994).
20. A. Takagi, K. Jinguji, M. Kawachi, "Wavelength Characteristics of (2 × 2) Optical Channel−Type Directional Couplers with Symmetric or Nonsymmetric Coupling Structures," J. Lightwave Technol. **10−6**, 735-746, (1992).
21. K. Færch, M. Svalgaard, "Symmetrical waveguide device fabricated by direct UV writing," IEEE Photonics Technol. Lett. **14**, 173-175, (2002).
22. S. Hewlett, J. Love, V. Steblina, "Analysis and design of highly broad-band, planar evanescent couplers," Opt. Quantum Electron. **28−1**, 71-81, (1996).
23. L. Leick, J. H. Povlsen, R. J. S. Pedersen, "Achieving small process tolerant wavelength-flattened 3dB directional couplers in Silica-on-Silicon," presented at Integrated Photonic Research 2000, Quebec City, Canada, July 2000.

1. Introduction

The capability of transferring power between waveguides is a key function for many applications of integrated optics. Directional couplers are considered building blocks of several systems, especially in optical networks, where they are deployed in devices such as switches, modulators and filters. The standard directional coupler is made of two identical waveguides that are coupled through the evanescent field, and its qualitative behavior is well described by coupled−mode theory [1]. Such a component exhibits considerable wavelength dependency which often limits the operational bandwidth to a few tens of nanometers, making it unsuitable for applications such as passive optical networking [2] where broadband performance is required. More recently a demand of broadband integrated optics has also appeared in fields such as near-infrared stellar interferometry, in which custom integrated optical components can effectively replace bulk optics [3]. Broadband directional couplers have been developed with several different designs, such as asynchronous coupling [4], interferometric structures [5], tapered couplers [6] and bent couplers [7]. For a 50% coupling ratio such designs have achieved a uniformity of ±2.5% (0.5 dB) over a bandwidth of 350-500 nm. However, these devices are often quite large and the fabrication involves many parameters that need optimization. This limits the integrability, decreases the production yield and increases the development cost. In addition fabrication techniques using photolithography are unsuitable for fabrication of custom components because the development process is long and expensive.

In this paper we report on broadband couplers fabricated by the direct UV writing technique [8], where waveguides are written directly into the photosensitive core of a planar, silica-based sample. Direct UV writing is well suited for low cost fabrication of broadband couplers because: 1) there is no need for photolithography and etching, 2) there is a unique capability to vary both waveguide index step and width by simply adjusting the applied scan velocity, 3) there are no overcladding step-coverage problems where voids are formed in the region between closely spaced cores [9,10] and 4) development of couplers with custom characteristics (coupling ratio, wavelength range, input/output spacing) is inexpensive and relatively fast. By employing an asynchronous coupler design that is optimized for UV writing we demonstrate a bandwidth up to 430 nm, total excess loss below 0.5 dB and a component length of ~8 mm. This combined performance exceeds what has previously been reported in the literature.

2. Device fabrication

The samples used in this work consist of three layer silica-on-silicon structures with a germanium/boron−doped photosensitive core layer. The thickness of the buffer/core/cladding is 16/5.4/12 μm. The core contains germanium and boron in a relative concentration so that

#8556 - $15.00 USD Received 23 August 2005; Revised 27 September 2005; Accepted 29 September 2005

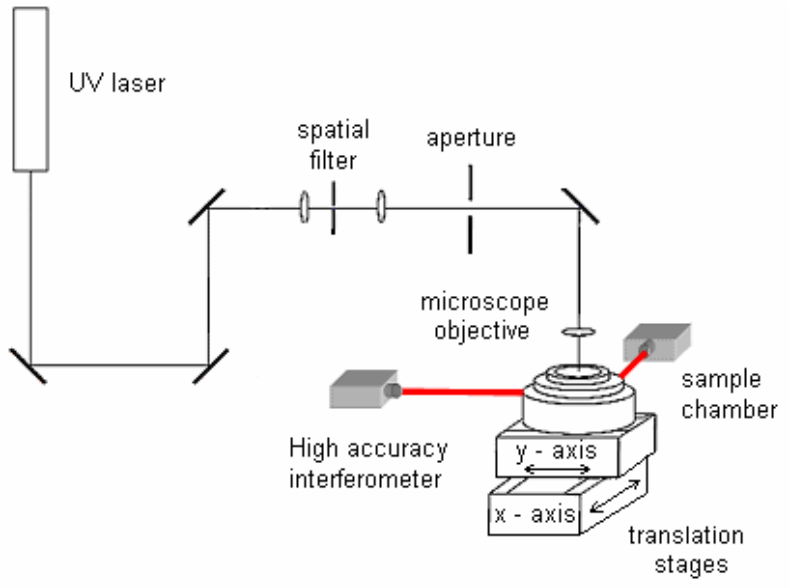

Fig. 1. Schematic drawing of the setup used for direct UV writing

the refractive index is matched (within $\pm 5\times10^{-4}$) to that of the surrounding layers [11]. The structure therefore does not support any guided modes before UV-writing. Index–matching the core layer enables the UV-written waveguides to exhibit a circular-mode profile and low coupling loss to standard telecom fiber [12]. Prior to UV exposure, the sample is loaded with molecular deuterium at a pressure of 500 bar until saturation to increase the photosensitivity [13].

The UV writing setup, similar to that used in previous work [14], is depicted in Fig. 1. The setup consists of a frequency doubled Ar^+ laser producing 257 nm radiation in a beam that is steered by several mirrors to a spatial filter / beam expander section. This produces a beam diameter of 5 mm which is focused by a microscope objective on the sample to a measured $1/e^2$ spotsize of 3.1 μm. The sample is housed in a small vacuum chamber with an antireflection-coated silica window where it is thermo-electrically cooled to −30 °C. This reduces the D_2 outdiffusion rate to negligible levels, ensuring that the photosensitivity is stable during UV writing [15]. Waveguides are written according to the desired layout by scanning the sample under the UV beam, using computer controlled, high-precision x-y translation stages. The main improvement in our current setup compared to earlier work [14] is that the position of the sample chamber is monitored using two double-step laser interferometers [16]. Two mirrors mounted on the vacuum chamber, parallel to the stage *x*–*y* axes, and at the same height as the sample, reflect a laser beam from each interferometer head. Detection of the resulting fringe pattern enables trajectory scan position feedback with 10 nm precision. The signal produced by the interferometer detection electronics is acquired through a PC card at a sampling rate of 25 Hz. In the old setup the position was measured inside the translation stages at a frequency of 5 Hz, with a precision of 0.1 μm and was susceptible to Abbe errors [17]. These improvements in position data have enabled a substantial improvement in the control over the trajectory scan process, resulting in a reduction of waveguide sidewall roughness and, consequently, a reduction of the propagation loss to a typical value of 0.02 dB/cm.

An incident UV power of 45 mW is used, which produces good waveguides for scan velocities in the range 40-2000 μm/s. After UV writing the samples are annealed at 80 °C for

#8556 - $15.00 USD Received 23 August 2005; Revised 27 September 2005; Accepted 29 September 2005

12 hours to outdiffuse residual D_2. The waveguide width has been measured with a Differential Interference Contrast (DIC) microscope while the peak index step has been measured by detecting interference fringes produced by the waveguide and its surrounding area upon illumination with semi–coherent light [18].

We have chosen to use a scan velocity of 280 μm/s for waveguide sections outside the central coupling region. After the 80 °C annealing the waveguide width and index step was measured to be 6.0 μm and 0.014, respectively. Single mode operation in both the 1300 nm and 1500 nm windows requires a lower index step and an additional annealing at 320 °C for 3 hours was therefore applied. This reduced the index step to 0.0085 with no change in width, which is suitable for operation in both telecom windows. The procedure of using a second annealing is quite normal for UV writing; it enables a standard UV processing scheme to be applied for a wide variety of structures after which the precise required index step can be chosen by adjusting the annealing time or temperature. An extra benefit of applying a second high temperature annealing is that it removes unstable components of the induced index change, thereby yielding devices with a very good degree of long term stability [19].

The variation of waveguide index step and width with scan velocity, after the high temperature annealing, is summarized in Fig. 2. Since both parameters vary with the scan velocity they cannot in this case be controlled independently. If such control is required then the incident UV power, in addition to the scan velocity, should be varied. For the lowest sampled scan velocity a 7.2 μm wide waveguide with an index step of 0.0092 is achieved. For larger scan velocities both the width and index step decreases. For a scan velocity of 2000 μm/s the resulting width is 3.3 μm while the index step has decreased to 0.006. Hence, by simply choosing a given scan velocity we can accurately control the width and index step of the resulting waveguide. This is a feature unique to UV writing and it will be utilized for fabrication of broadband couplers.

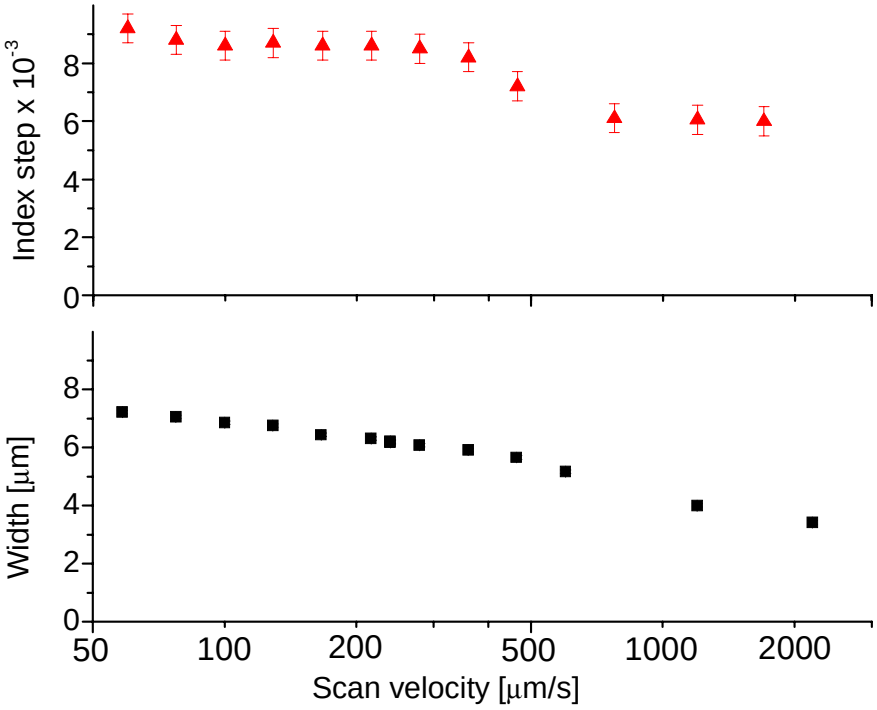

Fig. 2. Waveguide index step and width versus the applied scan velocity

#8556 - $15.00 USD Received 23 August 2005; Revised 27 September 2005; Accepted 29 September 2005

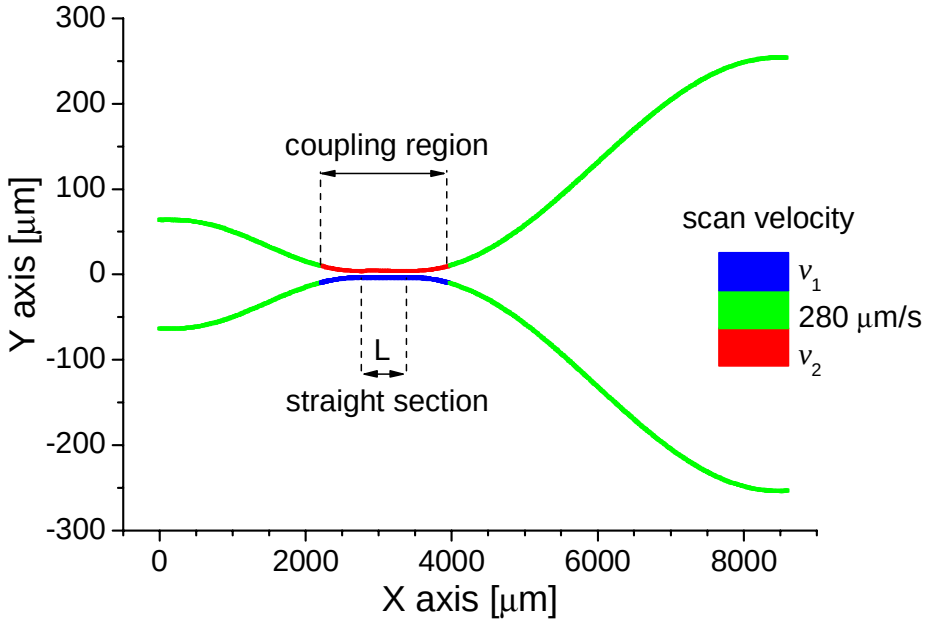

Fig. 3. Layout of a UV written broadband coupler. The arms of the coupler are written in two subsequent scans. The colors indicate the scan velocities applied in the different sections. The length of the straight section in the middle of the coupling region is chosen to achieve the desired coupling ratio

3. Coupler design

We have chosen to implement a design based on asynchronous coupling [4], i.e. a coupler with dissimilar waveguides in the central coupling region. The dissimilarity is achieved by choosing a different scan velocity for each arm in this region. First, an initial estimation of the parameters in the coupling section (step index, width and length of the coupled waveguides) is made based on coupled mode theory. Next, an experimental optimization is performed in order to define the layout parameters. The coupler that fulfills the design requirement is then reproduced in subsequent UV writing runs to validate the design. In section 3.1 the simplified theory of operation of an asymmetric coupler is briefly described, while in section 3.2 the method of implementation and layout details are given.

3.1 Asymmetric directional coupler: an approximated approach

The coupled mode theory summarized here is approximate because it relies on the fact that the field of the coupled waveguides is represented by the uncoupled mode fields as an orthonormal basis [1]. Under strong coupling this representation becomes inaccurate but many qualitative features of the simple description remain.

The normalized transferred power, P_2, between two straight waveguides of length L can be expressed as:

$$P_2 = F^2 \cdot \sin^2\left(\frac{C}{F}L\right) \tag{1}$$

#8556 - $15.00 USD Received 23 August 2005; Revised 27 September 2005; Accepted 29 September 2005

where C is the coupling coefficient and F is the cross coupling amplitude. The two terms depend on the mode overlap integral and on the waveguide index distribution. The wavelength−flattened operation is influenced by F^2, which reduces the dependence of the term $\sin^2$ with wavelength [20]. The wavelength dependency in (1) can be reduced by maximizing

1) the difference between the propagation constants of the coupled waveguides,
2) the coupling coefficient.

The condition 1) is achieved by varying the index step and/or the width of the two waveguides to get the desired coupling ratio, while the condition 2) is obtained by choosing the gap between the two waveguides to be small.

3.2 Layout

The layout of the broadband couplers is shown in Fig. 3. The separation of the input arms is 127 μm, which is compatible with commercially available fiber V-groove pigtailing technology. The output arms are spaced by 508 μm, so that the coupler later can be integrated with two 1×4 splitters to form a 2×8 optical splitter with an output port pitch of 127 μm. The input/output ports are connected to the coupling region through cosine S-bends. The use of cosine bends instead of circular bends deployed in previous work [21] reduces the component size while maintaining low loss.

The input/output bend lengths are 2.5 mm and 5 mm, respectively, yielding a minimum bend radius of ~20 mm. Measurement of concatenated bends have shown an excess loss of ~0.05 dB per S-bend. In the coupling region the scan velocity is decreased to v_1 (first arm) or increased to v_2 (second arm), in order to achieve an asynchronous coupling structure. In previous work [4] broadband performance was achieved from a similar structure where one waveguide was made narrower than the other. In our design this idea is extended since both the width and the index step decrease with scan velocity, thus increasing the difference in phase velocity between the waveguides. The waveguide center-to-center spacing in the central coupling region is fixed at 8 μm. The gap between the cores will therefore depend slightly on the applied scan velocities, since these control the waveguide widths (Fig. 2).

For the scan velocities reported in the following the gap can be as small as ~1.5 μm. This is significantly smaller than what is possible with etching based fabrication techniques [9,10] and ensures that the mode overlap integral becomes less sensitive to changes of the mode field diameter with wavelength [1]. The benefit of closely spaced cores is also numerically devised in [22]. The choice of v_1 and v_2 is related to the desired propagation constant in each waveguide, which is controlled by the width and index step (Fig. 2). A straight waveguide section in the middle of the coupling region is included so that a desired coupling ratio can be achieved by appropriately choosing the length.

The total coupler length is ~8 mm, which is 40−70% the length of that reported in previous demonstrations [4,6]. The UV writing time pr. coupler is short, typically around one minute, yielding a competitive and cost-effective technique for mass production.

4. Characterization

Device characterization is done using butt-coupled SMF-28 fiber and index matching oil for both input and output. The input fiber is connected either to a polarized 1557 nm source or an unpolarized broadband source operating in the range 1200-1750 nm. The insertion loss (IL) and polarization dependent loss (PDL) is measured with a dedicated IL/PDL measurement system at 1557 nm, while broadband measurements are performed on an optical spectrum analyzer.

Straight waveguides on a 15 mm long sample exhibit a total insertion loss of 0.1 dB and a polarization dependent loss (PDL) below 0.15 dB. Low insertion loss is possible due to reduced propagation loss mentioned in section 2 and low waveguide-fiber coupling loss (typically 0.03-0.04 dB/facet). The excess loss of the couplers compared to a straight waveguide is ~0.4 dB and the PDL is typically ~0.3 dB. This performance is better than that

#8556 - $15.00 USD Received 23 August 2005; Revised 27 September 2005; Accepted 29 September 2005

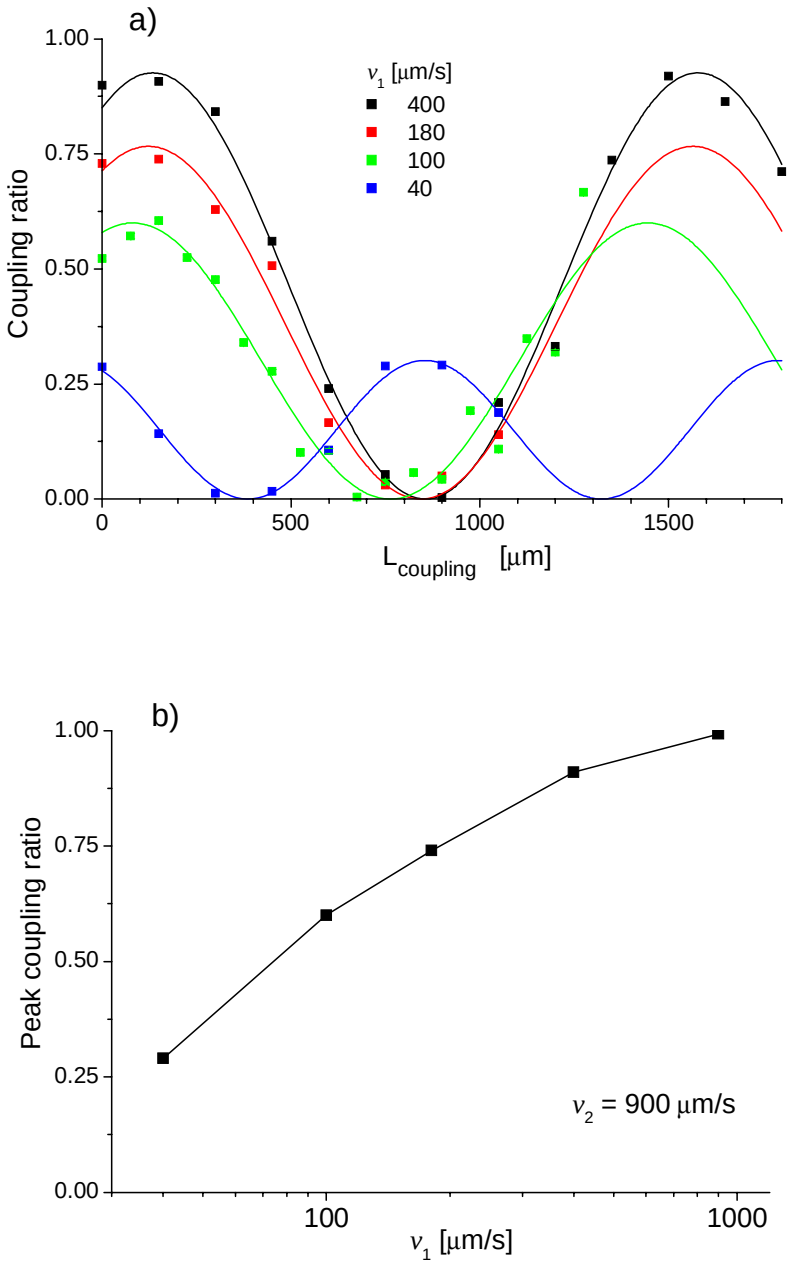

Fig. 4. (a) Measured coupling ratio at 1557 nm versus length of the straight section in the central coupling region for various velocities v_1 and a fixed velocity v_2=900 μm/s. For each dataset is fitted the $\sin^2$ behavior expected from coupled mode theory. (b) Peak coupling ratio versus the velocity of the first scan v_1.

#8556 - $15.00 USD Received 23 August 2005; Revised 27 September 2005; Accepted 29 September 2005

of similar devices fabricated with standard clean room technology [4] and curved couplers [7]. The losses are comparable to that of interferometric couplers [5] and to that of commercially available components as well.

Measurements at 1557 nm show the coupling ratio (the fraction of light transferred from the input waveguide to the other waveguide) varying in the expected sinusoidal way, as reported in Fig. 4(a). The uncertainty of the coupling ratio, due to measurement uncertainty of insertion loss, is below ±0.6%, and is thus indistinguishable on Fig. 4(a). The observed scattering around the fitted curves is most likely due to fabrication imperfections. The maximum attainable coupling ratio depends on the degree of synchronism of the coupled waveguides i.e. on the difference in terms of index step and width of the two cores. In Fig. 4(b) the peak coupling ratio is plotted versus the scan velocity v_1. As expected from coupled mode theory the peak coupling ratio increases toward unity for v_1 approaching v_2 (symmetric coupler). In earlier work (with different UV writing conditions) it was observed that an asymmetry could remain for $v_1=v_2$ due to a reduced photosensitivity in the vicinity of the first scan [21].

The typical device-to-device scattering in coupling ratio corresponds to a standard deviation of 1% (for a coupling ratio of 50%), while fabrication on different samples showed a standard deviation of 5%. The asymmetric coupler is tolerant to index step variations, but it is sensitive to waveguide dimensions [23]. In our setup the fluctuations of the waveguide width are mainly related to slow drift of the laser beam power. We expect to further increase the reproducibility of the couplers by actively stabilizing the laser power.

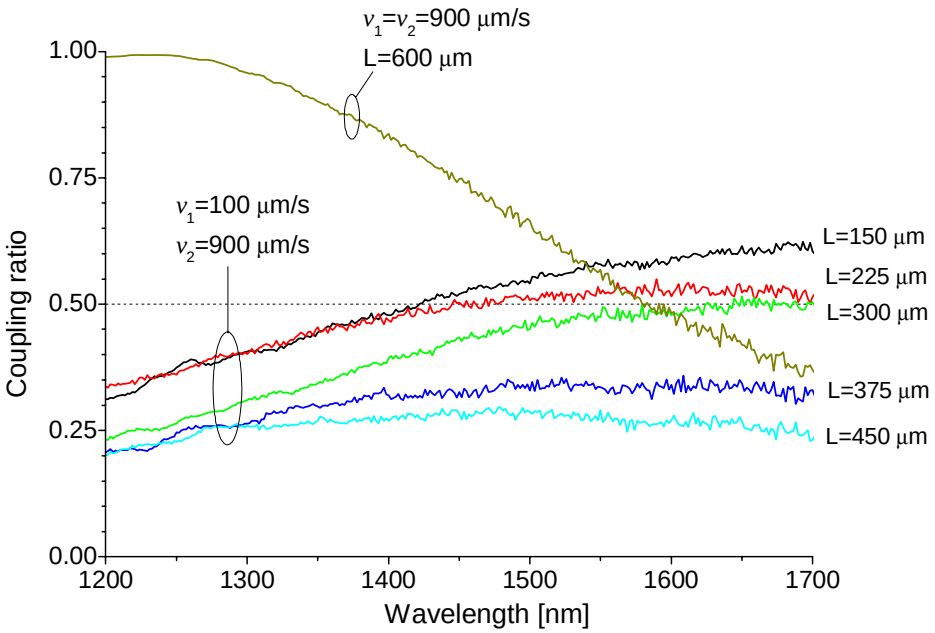

Fig. 5. Spectral variation of the coupling ratio for various asymmetric couplers. A measurement of a typical symmetric coupler is included for comparison.

5. Broadband performance

The broadband performance for a few selected couplers is shown in Fig. 5. The wavelength where maximum coupling occurs ranges from 1450-1750 nm, depending on the chosen coupling length. Using other velocities than those represented in Fig. 5 (e.g. v_1=40 μm/s,

#8556 - $15.00 USD Received 23 August 2005; Revised 27 September 2005; Accepted 29 September 2005

v_2=430 μm/s) we have made couplers with peak coupling wavelengths in the range 1300-1600 nm.

The peak coupling wavelength has been adjusted by experimental optimization to get the flat region of the wavelength response (i.e. the peak of the curve) in the desired spectral window. If the operational wavelength range is defined by requiring a flatness of 0.5 dB the selected couplers exhibit a bandwidth that ranges from 180 nm to 420 nm. This bandwidth is comparable to that achieved using much larger and more complicated structures [5,6], and better than the bent couplers recently fabricated [7]. In order to compare a broadband coupler with a standard symmetric coupler, the wavelength response of a component with both waveguides written at 900 μm/s is also plotted in Fig. 5. Using the same flatness requirement (0.5 dB) as before it is seen that the symmetrical coupler has a bandwidth of just ~30 nm at a 50% coupling ratio.

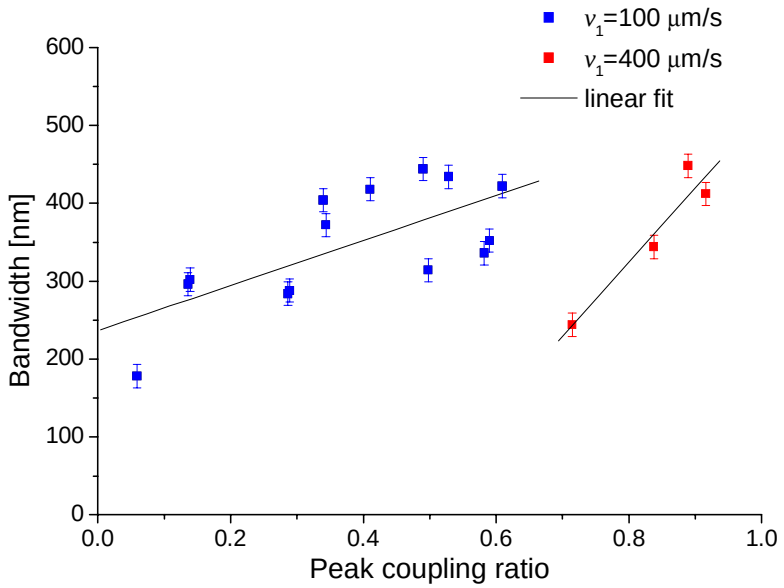

Fig. 6. Bandwidth for 0.5 dB flatness versus the peak coupling ratio for two different velocities v_1 (both with v_2=900 μm/s). The error bars correspond to a measurement uncertainty of ±15 nm. Each dataset is fitted with a straight line to highlight the trend.

The dependence of the coupling ratio with wavelength is contained in both factors of Eq. (1). A change in the coupling length affects the $\sin^2$ factor, changing the position of its peak, thereby varying the value of peak coupling ratio and the bandwidth. The flattest wavelength response for fixed values of the waveguides dimensions (i.e. fixed values of F and C) is achieved when the peak of the $\sin^2$ factor is at the same position of the maximum of F^2, so that the overall function reaches the highest grade of flatness. In other words the couplers that lie on the peaks of Fig. 4(a) have the best performance. This behavior is depicted in Fig. 6, where two datasets show the variation of bandwidth with the peak coupling ratio. One dataset is for v_1=100 μm/s while the other is for v_1=400 μm/s. Both have v_2=900 μm/s. The increasing trend of each dataset is highlighted by a straight line. The uncertainty on the bandwidth measurement is ±15 nm. It is clear that a large asymmetry (low v_1) produces a bandwidth that changes less with peak coupling ratio. Hence, a large degree of asymmetry lowers the sensitivity of the bandwidth to fabrication imperfections. Direct UV writing is

#8556 - $15.00 USD Received 23 August 2005; Revised 27 September 2005; Accepted 29 September 2005

especially well suited for producing large asymmetries since both the width and the index step can be locally controlled.

6. Conclusion

Broadband integrated optical waveguide couplers have been demonstrated using the direct UV writing technique. Wavelength-flattened performance is reported for a wide range of coupling ratios. Bandwidths up to ~430 nm have been achieved with a spectral flatness of 0.5 dB. The fabricated components exhibit low coupling loss to standard optical fiber (~0.03 dB/facet), low total excess loss (~0.5 dB) and low polarization dependency (0.3 dB). The couplers are compact (~8 mm long) and require only one minute of UV writing time. By employing a coupler design optimized for UV writing the combined performance in terms of bandwidth, loss and size exceeds what has previously been reported in the literature. The design is flexible and can easily be modified by choosing different scan velocities in order to move the band of operation to the desired wavelength range.

#8556 - $15.00 USD Received 23 August 2005; Revised 27 September 2005; Accepted 29 September 2005